Chapter 24

Live Cell Imaging of Endosomal Trafficking in Fungi

Sebastian Baumann, Norio Takeshita, Nathalie Grün, Reinhard Fischer, and Michael Feldbrügge

Abstract

Endosomes are multipurpose membranous carriers important for endocytosis and secretion. During membrane trafficking, endosomes transport lipids, proteins, and even RNAs. In highly polarized cells such as fungal hyphae, they shuttle bidirectionally along microtubules mediated by molecular motors like kinesins and dynein. For in vivo studies of these highly dynamic protein/membrane complexes, advanced fluorescence microscopy is instrumental. In this chapter, we describe live cell imaging of endosomes in two distantly related fungal model systems, the basidiomycete *Ustilago maydis* and the ascomycete *Aspergillus nidulans*. We provide insights into live cell imaging of dynamic endosomal proteins and RNA, dual-color detection for colocalization studies, as well as fluorescence recovery after photobleaching (FRAP) for quantification and photo-activated localization microscopy (PALM) for super-resolution. These methods described in two well-studied fungal model systems are applicable to a broad range of other organisms.

Key words Endosomes, Rab5, Microtubules, mRNA transport, RNA live imaging, Dual-color microscopy, FRAP, PALM, Ascomycete, Basidiomycete

1 Introduction

The vast majority of fungi grow in the form of hyphae, which are highly polarized cells like neurons and pollen tubes. Cellular processes at their growth apex are optimized for efficiency in order to deliver new building blocks for the cell membrane and enzymes for cell wall biosynthesis as well as hydrolytic enzymes enabling nutrition [1, 2]. Essential for polar growth is a highly sophisticated machinery for membrane trafficking. Secretory vesicles, for example, accumulate at the hyphal tip in high quantity for fusion with the plasma membrane. In addition to exocytosis, endocytosis plays an important role in polar growth [3, 4]. Endocytosis is important for recycling of membranes and membrane-bound proteins and could be involved in the organization of cell-end marker proteins at the tip [4–6]. After internalization, such endosomes shuttle bidirectionally by the action of molecular motors with opposite

directionality: minus end-directed dynein and plus end-directed kinesins such as Kin3/UncA [7–10]. Hyphae serve as excellent model systems to study membrane dynamics, because they provide sufficient resolution to perform the studies in a single cell. Compartments like nuclei, ER, and mitochondria are clearly resolvable, and endosomes are transported over long distances. In this chapter, we focus on two distantly related fungi, the basidiomycete *Ustilago maydis* and the ascomycete *Aspergillus nidulans*, which share a comparable machinery for long-distance membrane trafficking [8, 9, 11].

U. maydis is a pathogen that infects corn [12]. Prerequisite for infection is the mating of two yeastlike cells that form a filamentously growing dikaryon. The transcription factor bE/bW is the master regulator for the switch to polar growth. Its activity is regulated at the level of heterodimerization with subunits derived from different mating partners [12]. This knowledge allowed the generation of laboratory strains, in which the expression of an active bE/bW heterodimer is under control of a nitrate-regulated promoter. Thus, switching the nitrogen source results in efficient and synchronous elicitation of hyphal growth (Fig. 1a, b; *see* below).

Active microtubule-dependent transport of endosomes, which are positive for the small G protein Rab5a and the SNARE Yup1, is essential for efficient hyphal growth [7, 8]. A key factor for the function of these endosomes is the RNA-binding protein Rrm4

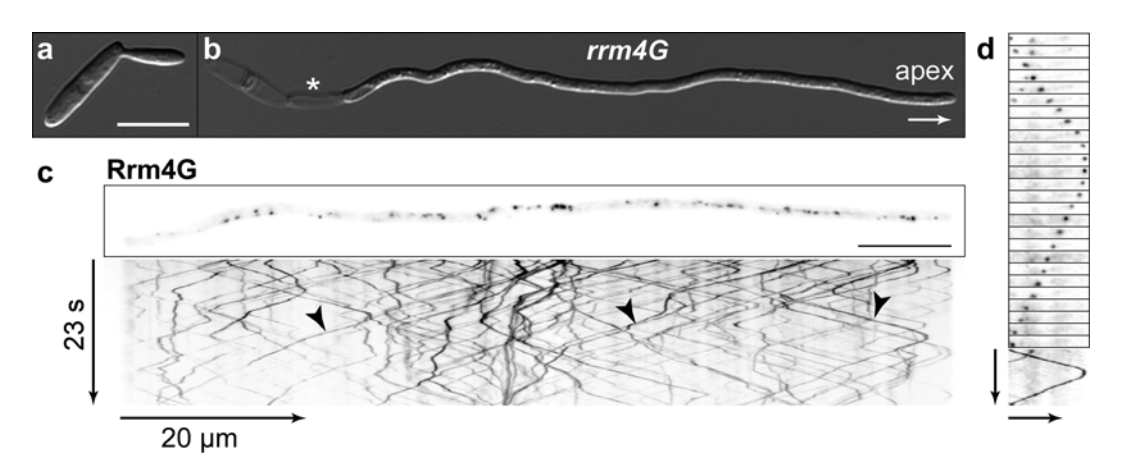


Fig. 1 Moving endosomes decorated with Rrm4G in hyphae of *U. maydis*. (a) Budding cell of *U. maydis* strain AB33rrm4G. (b) Hypha of AB33rrm4G, expressing Rrm4 fused to eGfp, 7 h after induction of hyphal growth; *arrow* indicates direction of growth, *asterisk* marks latest basal empty section. (c) Principle of a kymograph: (top) individual frames of a movie containing a selected region with a single Rrm4-decorated endosome moving forth and back. (*Bottom*) In a kymograph time on *Y*-axis plotted against the distance on *X*-axis, the Rrm4G signal is compressed to a single pixel on *Y*-axis (*vertical arrow*=7.6 s, *horizontal arrow*=5 μ m). (d) Fluorescence micrograph of Rrm4G. Depicted is the first frame of a movie (*top*) with corresponding kymograph (*bottom*). Kymographs were generated from movies with 150 ms exposure time (*inverted contrast*, bars=10 μ m). *Arrowheads* indicate Rrm4-positive endosomes shuttling in both directions

that mediates endosomal transport of mRNAs and ribosomes most likely to guarantee translation throughout the entire length of the hypha [13–15]. Importantly, Rrm4 also mediates endosome-coupled translation of specific mRNAs such as *cdc3* mRNA for loading of endosomes with septin. The translation product is delivered by these endosomes to the hyphal tip for correct assembly into higher-order septin filaments [14]. Thus, these endosomes are versatile multipurpose carriers transporting not only obvious cargo such as lipids but also cytoskeletal components, ribosomes, and mRNAs.

The ascomycete A. nidulans is an excellent model system for filamentous fungi. It completes the asexual life cycle, starting from a single conidiospore, within 24 h and is well suitable for genetic screens [16]. These resulted in the discovery of important eukaryotic factors such as the first eukaryotic tubulin genes-including γ -tubulin [17, 18]. Furthermore, the kinesin motor bimC was the founding member for a whole class of mitotic kinesins, and, last but not least, the isolation of nuclear distribution mutants (nud) revealed important insights into the human disease lissencephaly [19, 20]. In recent years, A. nidulans became an attractive model to study polar growth. The multinucleated hyphal tip compartment grows remarkably fast (about 0.5 µm/min) in an actin- and microtubule-dependent manner [21]. This growth speed depends on the predominant secretion of vesicles at the apex and also on endocytosis, which is required for membrane recycling. Its essential role was shown with different mutants of the endocytotic machinery, e.g., fimbrin (an F-actin cross-linking protein that plays a role in endocytotic internalization) and ArfB (a small GTPase) that leads to polarity defects [22, 23]. Shuttling Rab5-positive endosomes can be labeled with two paralogues RabA and RabB. These endosomes show characteristic long-distance bidirectional movement on microtubules, driven by the corresponding motor proteins dynein and most likely a kinesin-3 type motor UncA [10, 24, 25].

Here, we describe important techniques for live cell imaging of endosomal trafficking such as (1) millisecond alternating laser excitation (msALEX) for dual-color acquisition applied during in vivo colocalization studies on moving endosomes. msALEX allows for the alternating excitation of different fluorophores with a minor time shift, but with the advantage of a longer observation time because of reduced bleaching of the respective fluorophores. (2) RNA live imaging to demonstrate endosomal mRNA transport [13, 14, 26] relies on the insertion of binding sites for a specific peptide derived from a heterologous RNA-binding protein like λ N in the 3' untranslated region (UTR) of the mRNA of interest. Thereby, the localization of these mRNAs can be visualized by expressing a fusion protein consisting of λ N-Gfp, because the fluorescent protein is specifically recruited to these mRNAs. (3) FRAP (fluorescence recovery after photobleaching) is used to

quantify the interaction of endosomal cargo with proteins at the final destination [14]. (4) PALM (photo-activated localization microscopy) uses photoswitchable fluorophores to achieve temporal control of the emission. The fluorophore is converted between a fluorescent ("on") state and a dark ("off") state or states that fluoresce at different wavelengths, such as photoconversion from green to red fluorescence. Therefore, when activation light of a sufficiently low intensity is applied to the sample, only a random, sparse subset of fluorophores is activated to the on or red fluorescent state at any time, allowing these molecules to be imaged individually. Signals can be precisely localized and then deactivated by switching to a reversible dark state or permanent bleaching. Repetitive cycles of activation, imaging, and deactivation allow the construction of super-resolution images [27]. One fluorescent protein, mEosFP, can be photoconverted from green to red fluorescence by 400 nm light [28]. The red signals of mEosFP activated at random are used during PALM imaging. Here, we show a PALM analysis of TeaR, a membrane-associated cell-end marker that controls the growth direction of hyphae by focusing polarity markers at the growing tip [6, 29].

2 Materials

2.1 Preparing Hyphae for Live Cell Imaging

Ustilago maydis

- 1. Complete medium (CM): 0.25 % (w/v) casamino acids (Difco), 0.1 % (w/v) yeast extract (Difco), 1.0 % (v/v) vitamin solution, 6.25 % (v/v) salt solution, 0.05 % (w/v) herring sperm DNA (Sigma), and 0.15 % (w/v) NH₄NO₃; add H₂O_{bid.}, adjust pH with 5 M NaOH to 7.0, and add glucose (glc) or arabinose (ara) solution after autoclaving (1 % f.c.).
- 2. Nitrate minimal medium (NM): 0.3 % (w/v) KNO₃, 6.25 % (v/v) salt solution.
- 3. Vitamin solution: 0.1 % (w/v) thiamine hydrochloride, 0.05 % (w/v) riboflavin, 0.05 % (w/v) pyridoxine, 0.2 % (w/v) calcium pantothenate, 0.05 % (w/v) p-aminobenzoic acid, 0.2 % (w/v) nicotinic acid, 0.2 % (w/v) choline chloride, 1 % (w/v) *myo-inositol*; add H_2O_{bid} , and sterile filtration.
- 4. Salt solution: 16 % (w/v) KH₂PO₄, 4 % (w/v) Na₂SO₄, 8 % (w/v) KCl, 1.32 % (w/v) CaCl₂×2 H₂O, 8 % (v/v) trace elements, 1 % (w/v) MgSO₄ (water free); add H₂O_{bid.}, and sterile filtration.
- 5. Trace elements: 0.06% (w/v) H_3BO_3 , 0.14% (w/v) $MnCl_2\times 4$ H_2O , 0.4% (w/v) $ZnCl_2$, 0.4% (w/v) $Na_2MoO_4\times 2$ H_2O , 0.1% (w/v) $FeCl_3\times 6$ H_2O , 0.04% (w/v) $CuSO_4\times 5$ H_2O ; add H_2O_{bid} , and sterile filtration.
- 6. Glass reaction tubes, baffled flasks 125 ml.

Aspergillus nidulans

- 1. Minimal medium: 5 % (v/v) salt solution, 0.1 % (v/v) trace elements, 2 % (w/v) glucose or 2 % (v/v) glycerol; add $\rm H_2O_{bid.}$, and adjust pH with 10 M NaOH to 6.5.
- 2. Salt solution: 12 % NaNO₃; 1 % KCl, 1 % MgSO₄×7H₂O, 3 % KH₂PO₄; add H₂O_{bid}.
- 3. Trace elements: 2.2 % ZnSO₄×7H₂O; 1.1 % H₃BO₃; 0.5 % MnCl₂×4H₂O; 0.5 % FeSO₄×7H₂O; 0.16 % CoCl₂×5H₂O; 0.16 % CuSO₄×5H₂O; 0.11 % (NH₄)₆Mo₇O₂₄×4H₂O; 5 % Na₄-EDTA; adjust pH with 10 M KOH to 6.5.
- 4. Glass-bottom FluoroDish (World Precision Instruments, Berlin, Germany).

2.2 General Microscopy Equipment for Live Cell Imaging

- 1. Wide-field-fluorescence microscope (Axio Observer.Z1, Zeiss, Jena, Germany).
- 2. Metal-halide lamp or laser for excitation of eGfp (488 nm/50 or 100 mW) or Rfp/mCherry (561 nm/50 or 150 mW).
- 3. Filter sets (eGfp ET 470/40×, ET525/50 m, T495_PXR and mCherry ET560/40×, ET 630/75 m, T585lp, AHF Analysentechnik, Tübingen, Germany).
- 4. Zeiss objectives: Plan-Apochromat (63×, NA 1.4) and EC Plan-Neofluar (100×, NA 1.3).
- 5. CoolSNAP HQ2 CCD camera (Photometrics, Tucson, AZ, USA).
- 6. Software package MetaMorph (version 7, Molecular Devices, Sunnyvale, CA, USA).
- 7. VisiFRAP 2D control software for Meta Series 7.6 (Visitron Systems, Munich, Germany) to adjust laser excitation power.
- 8. Microscope slides 76×26 mm (Marienfeld, Lauda-Königshofen, Germany).
- 9. High precision cover slips 18×18 mm, $D=170 \pm 5$ μ m (Zeiss, Jena, Germany).
- 10. Agarose (Bio-Rad, Munich, Germany).

2.3 Microscopy Equipment for Local Photobleaching and Dual-Color Acquisition

- A VS-LMS4 Laser-Merge-System (Visitron Systems, Munich, Germany) with solid-state lasers for excitation of eGfp (488 nm/50 or 100 mW) and Rfp/mCherry (561 nm/50 or 150 mW).
- 2. Multiband filter set for eGfp/mCherry (59022, Chroma, Bellows Falls, VT, USA).
- 3. VisiFRAP 2D-System (Visitron Systems, Munich, Germany) including a 405 nm/80 mW diode laser, regulated by a UGA-40 controller (Rapp OptoElectronic GmbH, Hamburg, Germany).
- 4. VisiFRAP 2D control software for Meta Series 7.6 (Visitron Systems, Munich, Germany).

2.4 FRAP Setup

- 1. 40× EC Plan-Neofluar objective (NA 1.3, Zeiss, Jena, Germany).
- 2. 472 nm LED (CoolLED, precisExcite, Andover, UK) (see Note 1).
- 3. See items 3 and 4 in Subheading 2.3.
- 4. PIFOC P-737 high-speed Piezo Z-stage (Physik Instrumente GmbH & Co. KG, Karlsruhe, Germany).
- 5. Software-driven autofocus.

2.5 PALM Setup

- 1. Modified inverted microscope (Axiovert 200, Zeiss, Jena, Germany) equipped with a 63× C-Apochromat water immersion objective (NA 1.2, Zeiss, Jena, Germany).
- 2. Three diode-pumped solid-state lasers, with wavelengths 561 nm/up to 150 mW (Cobolt Jive, Cobolt, Solna, Sweden), 473 nm/up to 600 mW (LSR473-200-T00, Laserlight, Berlin, Germany), and 405 nm/up to 150 mW (CLASII 405-50, Blue Sky Research, Milpitas, CA, USA) for excitation and photoactivation of the fluorophores.
- 3. Excitation dichroic (z 405/473/561/635, AHF, Tübingen, Germany), band-pass filter for emission (607/50, AHF, Tübingen, Germany).
- 4. Back-illuminated EMCCD camera (iXon Ultra 897, Andor, Belfast, Northern Ireland).
- 5. Appropriate dichroic mirrors (AHF, Tübingen, Germany) and AOTF (AOTFnC-400.650, A-A, Opto-Electronic, Orsay Cedex, France).
- 6. Single-mode fiber (OZ Optics, Ottawa, Ontario, Canada).
- 7. Custom-written analysis software, a-livePALM, ran in MATLAB R2010b (The MathWorks, USA) environment [30].
- 8. Personal computer using an Intel(R) Core™ i7-2600 processor clocked at 3.4 GHz with 8 GB memory. A NVIDIA GeForce GTX 560 Ti graphics card with 1 GB memory was used for GPU-based computation.

3 Methods

An important prerequisite for live cell imaging in fungal model systems is the generation of transgenic strains expressing the proteins of interest fused N- or C-terminally to fluorescence proteins such as the green and red fluorescent protein (eGfp or mRfp). Preferably, this is achieved by integration at the homologous locus in order to avoid overexpression artifacts. To this end, sophisticated strategies have been described [31, 32]. Alternatively, it is

possible to express the protein ectopically in addition to the wild-type version at defined loci such as the *ip*^s locus in *U. maydis* [33] (*see* **Note 2**). Importantly, it needs to be verified that the expression of fusion proteins are functional and do not cause altered hyphal growth (Fig. 1a, b). The test can be easily done by complementation of a deletion mutant with the construct of interest, if it is a nonessential gene and if deletion causes a phenotype. Full complementation of the mutant phenotype is desired.

3.1 Live Cell Imaging of Dynamic Endosomes in U. maydis

- 1. Inoculate 3 ml of CM-glc (1 % f.c.) in a glass tube and grow on wheel incubator for 20–24 h at 28 °C.
- 2. Dilute cells 1:5,000 in 30 ml of CM-glc (*see* **Note** 3), and incubate for 17–18 h in a 125 ml baffled flask shaking at 200 rpm and 28 °C.
- 3. Adjust OD₆₀₀ to 0.5 (final volume 20 ml), and shift the cells to NM-glc by centrifugation at 3,500×g for 3 min (*see* Note 4). Wash once in NM-glc, centrifuge again, and resuspend in 20 ml NM-glc. Transfer cells into a new 125 ml baffled flask.
- 4. Pipette about 300 µl of 3 % liquid agarose on a microscope slide. Immediately place a second slide on the agarose drop, perpendicular to the lower slide. Remove one microscope slide by sliding it slowly sideways. This results in a thin agarose cushion on the microscope slide (*see* Note 5).
- 5. Pipette 0.3 μl of cell suspension onto the cushion, let it dry for 1 min, and position cover slip on top.
- 6. To visualize endosomes in whole hyphae, use a 63× objective and full camera frames (*see* **Note** 6).
- 7. Choose appropriate illumination for excitation of fluorophores (metal-halide lamp or laser) and filter sets (excitation/emission/dichroic beam splitter).
- 8. Drive camera in stream mode with 150 ms exposure time and in overlapping exposure and readout mode ("normal" mode) to obtain the fastest acquisition (*see* **Note** 7).
- 9. Convert resulting movie into a kymograph (Fig. 1c, d; see Note 8).
- 10. Analyze kymographs for endosome behavior such as direction of movement, pausing events, velocity, and turning frequency.

3.2 Live Cell Imaging of Dynamic Endosomes in A. nidulans

- 1. Inoculate spores from colony in 0.5 ml minimal medium (about 10³ spores per ml) with 2 % glycerol (derepression of the *alcA* promoter) mounted on a sterile cover slip. Incubate the cells for 16–20 h at 28 °C for germination and hyphal growth (Fig. 2a; *see* Note 9).
- 2. Mount the cover slips upside down on a microscope slide.

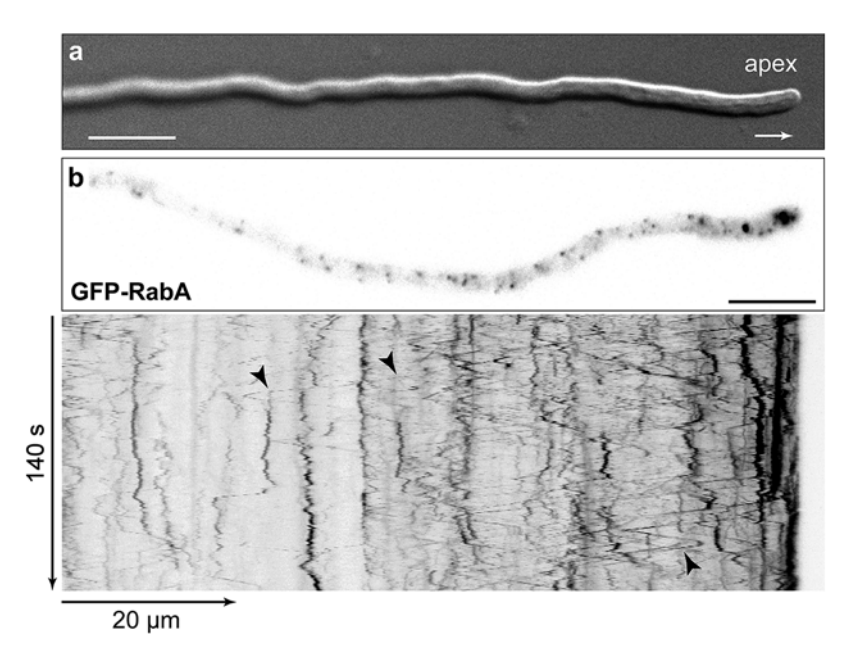


Fig. 2 Moving endosomes decorated with Gfp-RabA in hyphae of *A. nidulans*. (a) DIC image of *A. nidulans* hyphae. (b) Fluorescence micrograph of RabA tagged with Gfp. Depicted is the first frame of a movie (*top*) with corresponding kymograph (*bottom*). Kymographs were generated from movies with 450 ms exposure time (*inverted contrast*). *Arrowheads* indicate RabA-positive endosomes shuttling in both directions. Scale bars = 10 µm

- 3. To visualize endosomes, use the 63× objective and an appropriate camera frame to visualize the whole hypha.
- 4. Choose appropriate illumination for excitation of fluorophores, and filter sets (excitation/emission/dichroic beam splitter) and exposure time.
- 5. Drive camera in stream mode to obtain the fastest acquisition.
- 6. Convert resulting movie into a kymograph (Fig. 2b).
- 7. Analyze kymograph for endosome behavior like direction of movement, pausing events, speed, and turning frequency (*see* **Note 10**).
- 3.3 Colocalization of Proteins at Dynamic Endosomes Using Dual-Color Acquisition
- 1. Follow steps 1–6 in Subheading 3.2 (see Notes 11 and 12).
- 2. Use a 63× or 100× objective, without or with camera chip binning 2, respectively (*see* **Notes 6** and 7).
- 3. Alternating laser excitation is operated by the microscope control software (*see* **Note 13**).
- 4. Drive camera in stream mode with 80 ms exposure time for each fluorophore and in overlapping exposure and readout mode to obtain the fastest acquisition, and choose region of interest (see Notes 7 and 14).

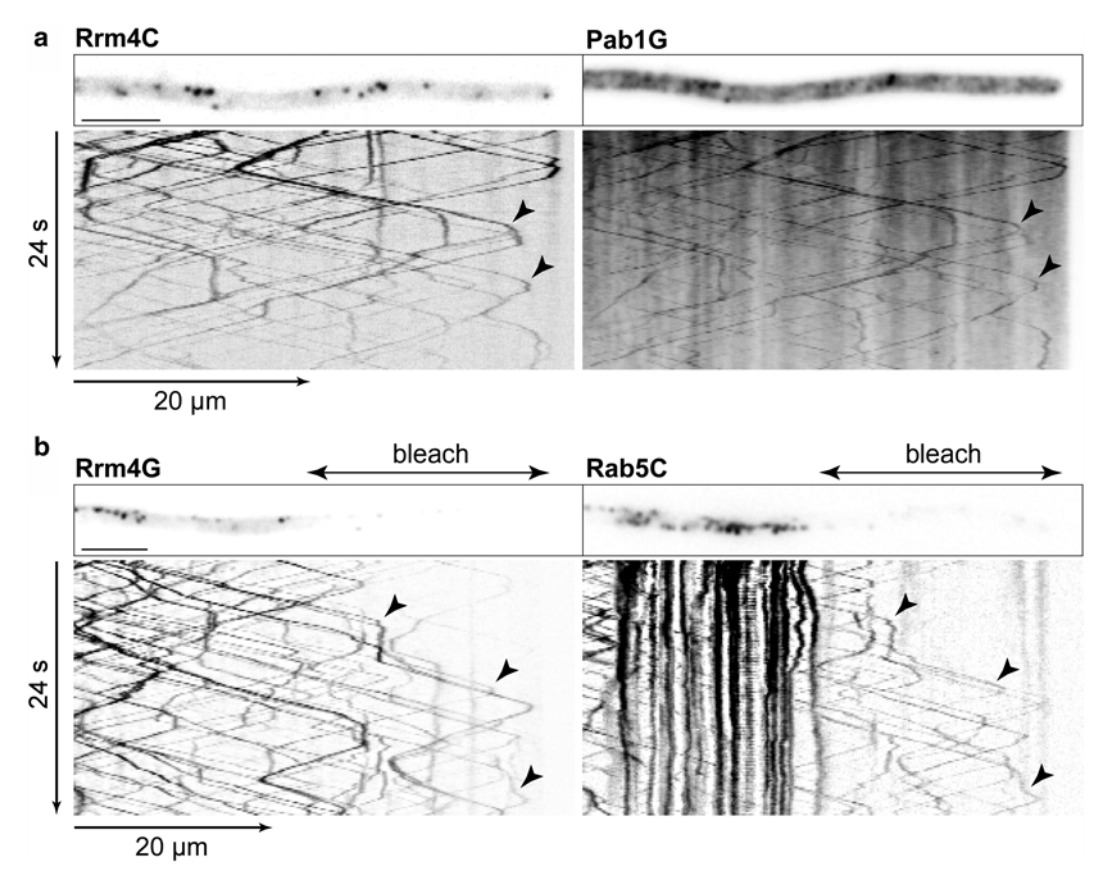


Fig. 3 Colocalization of proteins on dynamically moving endosomes. (a) Dual-color acquisition with msALEX of hypha expressing RrmC and Pab1G. Kymographs were generated from a movie that was acquired with a 63×0 objective and 80 ms exposure time per fluorophore. (b) Dual-color acquisition with local photobleaching followed by msALEX of hypha expressing Rrm4G and Rab5aC. Kymographs were generated from a movie that was acquired with a 100×0 objective, 80 ms exposure time per fluorophore, and camera chip binning 2; prior to acquisition, the indicated area was photobleached

- 5. Adjust laser intensity (*see* **Note 15**).
- 6. Convert resulting movies into kymographs (Fig. 3; see Note 8).
- 7. Analyze kymographs for protein colocalization (see Note 16).

3.4 RNA Live Imaging

- 1. Generate the λN^* -Gfp² fusion construct (Fig. 4a, b; see Note 17).
- 2. Insert *boxB* hairpins into the 3' UTR of your gene of interest (Fig. 4a, b; *see* Note 18).
- 3. Transform both constructs successively into *U. maydis*. Verify correct strain generation by Southern blot analysis.
- 4. Inoculate 3 ml of CM-glc (1 % f.c.) in a glass reaction tube for 20–24 h at 28 °C on an incubation wheel.
- 5. Dilute cell culture 1:2,500 in 30 ml of CM-ara (1 % f.c.; see Notes 3 and 19), and regrow in a baffled flask for 18 h at 200 rpm and 28 °C.

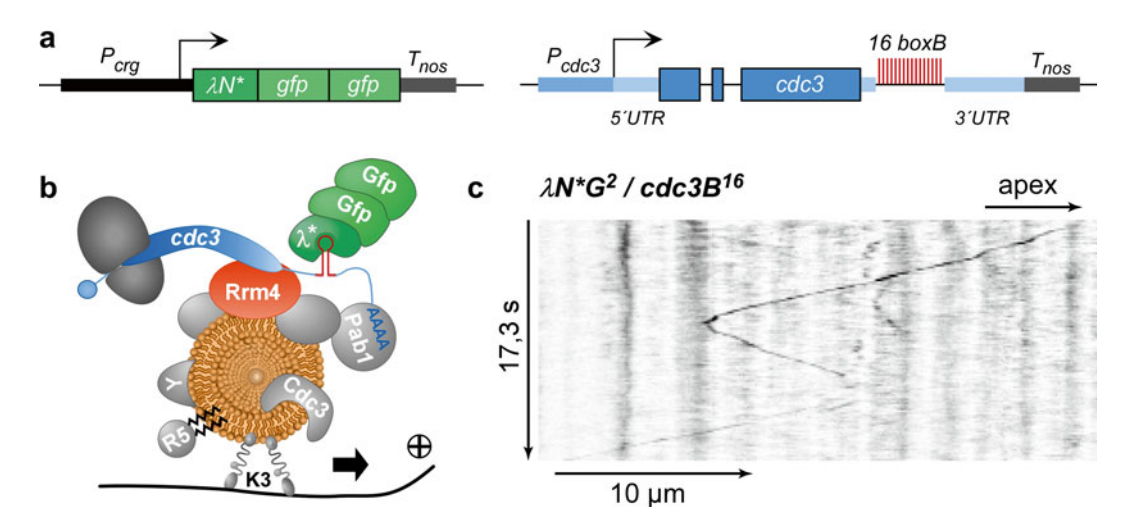


Fig. 4 λ N-based RNA live imaging in *U. maydis*. (a) Schematic representation of constructs: the gene encoding the λ N*-peptide fused to tandem eGfp is under control of the arabinose-inducible *crg1* promoter (*left*; T_{nos} = heterologous terminator); the *cdc3* gene is tagged with 16 copies of the λ N*-binding sites *boxB* in its 3' UTR (*right*). (b) Schematic representation illustrating the concept of RNA live imaging: the λ N*G² fusion protein is recruited to the *cdc3* mRNA via *boxB* binding sites (for the sake of simplicity, only a single interaction is shown), the Rrm4 links this complex to endosomes which are transported via molecular motors along microtubules, and different endosomal cargos are indicated, *R5* Rab5a, *Y*Yup1, and *K3* Kin3. (c) Kymograph showing shuttling *cdc3B*¹⁶ mRNA labeled with λ N*G²

- 6. Adjust OD₆₀₀ to 0.5 (final volume 20 ml) and shift the cells to NM-ara by centrifugation at 3,500×g for 3 min (see Note 4). Wash once in NM-ara, centrifuge again, and resuspend in 20 ml NM-ara. Transfer cells into a new 125 ml baffled flask. Filamentous growth should be induced for at least 8 h prior to microscopic analysis.
- 7. Follow **steps 4–6** in Subheading 3.2.
- 8. Use a 63× objective or 100× with camera chip binning 2 (see Notes 6 and 7).
- 9. Follow steps 8–11 in Subheading 3.2 (Fig. 4c; see Note 20).

3.5 FRAP Experiments

- 1. Prepare hyphae of *U. maydis* expressing septin-Gfp-fusion protein Cdc3G according to **steps 1–6** in Subheading **3.2**.
- 2. Determine the minimum laser power necessary for bleaching the region of interest.
- 3. Operate camera in the most sensitive settings: set readout speed to 10 MHz to reduce readout noise (*see* **Note 21**), operate camera in "alternate normal" mode to provide best quantum efficiency, and set camera gain to 3.
- 4. Use 472 nm LED for illumination.

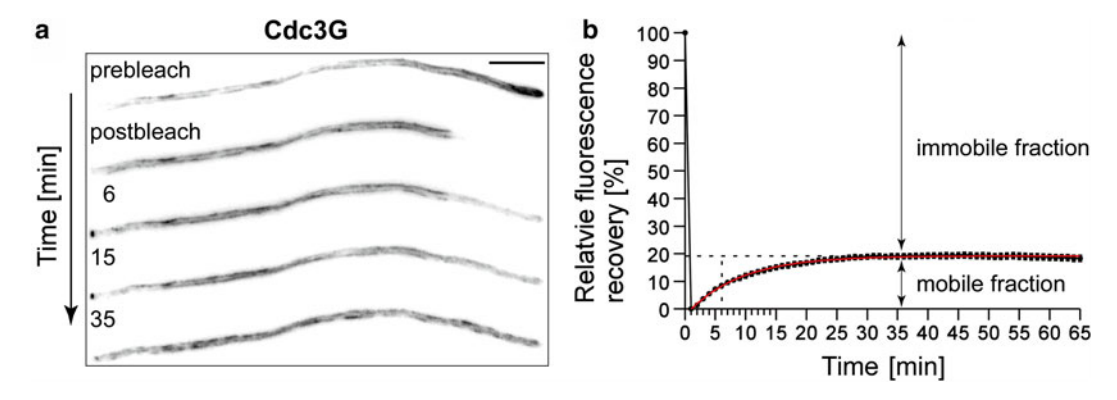


Fig. 5 FRAP of Cdc3G at hyphal tips of *U. maydis* (a) Fluorescence micrographs illustrating the chronology of a FRAP experiment: fluorescence recovery underlies endosomal transport of Cdc3G [14]; different steps and selected time points are indicated (bar = $10 \mu m$). (b) Fluorescence recovery is plotted against time, half-time recovery ($t_{1/2}$, *vertical dashed line*), and mobile as well as immobile fractions (*double arrows*) are deduced from the fitted curve (*red*), and *horizontal dashed line* indicates plateau

- 5. Before bleaching, take a *z*-stack of 10 planes with an exposure time of 500 ms and a distance between single planes of 0.5 μm (*see* **Note 22**).
- 6. Bleach 15 μ m of the hyphal tip in ten *z*-planes through fungal hyphae with a *z*-distance of 0.5 μ m.
- Immediately acquire fluorescence recovery in ten z-planes with an exposure time of 500 ms each with a z-distance of 0.5 μm (open camera shutter).
- 8. Take a z-stack every minute for a period of 65 min (Fig. 5a; see Notes 22 and 23).
- 9. For data analysis, convert all z-stacks to maximum projections and correct for drift of cells during the experiment (*see* **Note 24**).
- 10. Subtract average background in each image (see Note 25).
- 11. Determine the amount of acquisition bleaching and correct all images (*see* **Note 26**).
- 12. Normalize postbleach intensities to prebleach intensities, plot fluorescence recovery against time, apply curve fitting, and determine half-time recovery as well as mobile and immobile fraction of protein with Prism 5 software (GraphPad, Fig. 5b).

3.6 PALM Experiments

- 1. Inoculate spores of *A. nidulans* strain expressing mEosFP-TeaR in a glass-bottom chamber with minimal media. Incubate at 25 °C for 12 h.
- 2. With low 473 nm illumination, identify a cell that expresses a high level of fluorophores.
- 3. Adjust laser intensity to image mEosFP. Initially, illuminate the sample with the 561 nm laser to bleach the small population of mEosFP that is already converted, e.g., emits red fluorescence (*see* Note 27).

- Fluorescent proteins are converted one by one from their green to their red emitting forms using low intensity (0-50 W/cm²) 405 nm light and excited at 561 nm simultaneous illumination (200-400 W/cm²).
- 5. Use a 607/50 band-pass filter after passing through the excitation dichroic (z 405/473/561/635) to detect the red fluorescence.
- 6. Detect and record the signals from individual red fluorescent mEosFP molecules with a back-illuminated EMCCD camera typically at 50 ms time resolution (*see* **Note 28**).
- 7. Analyze the PALM data with custom-written analysis software, a-livePALM, ran in MATLAB R2010b environment [30]. Use the molecule identification threshold value, *P* value, of 0.04 to identify and fit all data (*see* **Note 29**).

4 Notes

- 1. We observed the lowest acquisition bleaching during recovery time using the 472 nm LED.
- 2. Different marker proteins are available in *U. maydis* to visualize endosomes: Rab5a, the SNARE Yup1, and the RNA-binding protein Rrm4. We recommend using Rrm4 as endosomal marker, as Rrm4 localizes exclusively to moving endosomes (Figs. 1d and 3b). In contrast, Rab5a and Yup1 stain additional structures.
- 3. Culture volume can be adjusted. The ratio for inoculation should be 1:5,000 at best. Do not exceed 1:1,000 since this might affect hyphal growth.
- 4. Some mutant strains might require an extended period of spinning at higher velocities, e.g., 5 min at $8,000 \times g$.
- 5. Agarose cushions ensure a plane orientation of hyphae in a single focal plane. We recommend drying the agarose for 10–20 min before usage.
- 6. Use high numerical aperture objectives, e.g., NA 1.3 or higher.
- 7. With these settings, frame rate equals exposure time. Endosomes in *U. maydis* move 2–3 μ m per second. Therefore, camera exposure time should not exceed 200 ms. If fluorescent signals are weak, choose a $100\times$ objective and apply binning to the camera chip.
- 8. Microscope equipment is controlled by MetaMorph (version 7), which is used to generate kymographs. Free software, e.g. ImageJ, is also available [34]. In a kymograph, the pixel with the highest intensity of each moving structure is plotted against time in a coordinate system. This results in a 2D projection of 3D data (Fig. 1c).

- 9. Use high precision cover slips $(170\pm 5~\mu m)$ to avoid intensity changes due to local thickness differences in your resulting image. For longtime imaging, use glass-bottom dishes with correct cover slip thickness (#1.5), and hyphae will stay healthy for an extended period of time.
- 10. Kymographs are generated using Zeiss software (Zen) or Fiji (ImageJ, [34]).
- 11. For slow processes, a metal-halide lamp combined with an excitation filter wheel or with the microscope filter turret is sufficient for colocalization studies.
- 12. If dual-color experiments are performed, objectives should be tested for chromatic aberrations. Usually objectives of the apochromat type are well corrected. We use a 100× EC-Neofluar objective (NA 1.3, Zeiss) that has no detectable shift in z-planes if Gfp and mCherry are visualized. Use commercially available fluorescent beads to test for chromatic aberrations.
- 13. In Subheading 2.4 (items 6 and 7), the applied software is listed.
- 14. We recommend exposure times no longer than 80 ms. Check the frame rate limit of your camera and choose a region of interest if required. Alternatively use a 100× objective with binning 2, which enhances signal intensity and allows shorter exposure times at the cost of resolution.
- 15. When performing msALEX, one should be aware that the 488 nm laser excites mCherry to a low degree. Depending on the expression level of the tagged protein, this might result in a moderate false-positive signal which can be detected with the dual emission filter. Therefore, in control experiments, the protein tagged with mCherry should be excited with 488 nm light without expressing a Gfp-fusion protein simultaneously. The degree of cross talk should be checked and laser intensity be adjusted accordingly.
- 16. If the protein of interest exhibits a cytoplasmic localization in addition to the endosomal localization, local photobleaching might be needed before dual-color acquisition. For photobleaching, a 405 nm laser is required. Identify a region of interest and bleach prior to acquisition (Fig. 3b).
- 17. The gene encoding the λN^* -peptide carries three point mutations derived from a related arginine-rich RNA-binding peptide of phage P22. The gene encoding λN^* -Gfp² is inserted at the ip^S locus. Expression is controlled by the arabinose-inducible promoter P_{crg1} .
- 18. With this setup, we are able to detect mRNAs under endogenous expression levels. RNA sequencing data on the MUMDB

- [35] help to determine the length of 3' UTRs; for tagging *cdc3* (um10503) mRNA, *boxB* hairpins were inserted 100 nt downstream of the stop codon.
- 19. At first, P_{crg1} is induced because switching on P_{nar1} and P_{crg1} promoters simultaneously results in a delay of filament induction.
- 20. Due to the relatively high cytoplasmic signal intensity of λN^*G^2 , we recommend to draw the line for the kymograph point by point to ensure the selection of the pixel with the highest intensity for the kymograph line. The thickness of the kymograph line should not exceed three pixels.
- 21. This setup is optimized for comparably slow fluorescence recovery processes in the order of minutes. For recovery in the order of seconds, settings have to be adapted for faster acquisition.
- 22. Before acquiring Gfp fluorescence with the LED, the software-driven autofocus was used in the DIC channel to assure that acquisition started in the correct focal plane. The whole procedure can be automated with the "multidimensional acquisition" tool of MetaMorph 7.
- 23. In our experiment, we determined fluorescence recovery of a cortical protein. Acquiring *z*-stacks might not be required if studying cytoplasmic proteins and are not applicable if recovery processes in the range of seconds are analyzed.
- 24. Shrinking of the agarose cushion requires drift correction.
- 25. Identify a background region of a certain size that can be used in all experiments.
- 26. With every z-stack taken, the Gfp fluorescence gets photobleached to a certain amount. One has to correct for this acquisition bleaching. Also correct for collateral bleaching. The high intensity of the 405 nm laser causes bleaching in areas outside the determined area.
- 27. A small population of mEosFP emits red fluorescence already before irradiation with 405 nm light. That is an original character of mEosFP.
- 28. As the pool of non-converted mEosFP is depleted during data acquisition, it is advisable to increase the power of the activation laser to keep the number of activated fluorophores per frame constant.
- 29. For a typical image size of 256×256 pixels per image in 16-bit tif format, the processing time is 15–30 ms per image, depending on the complexity of constructed image. The PALM micrograph in Fig. 6a is constructed by 1,000 frames with a time resolution of 50 ms.

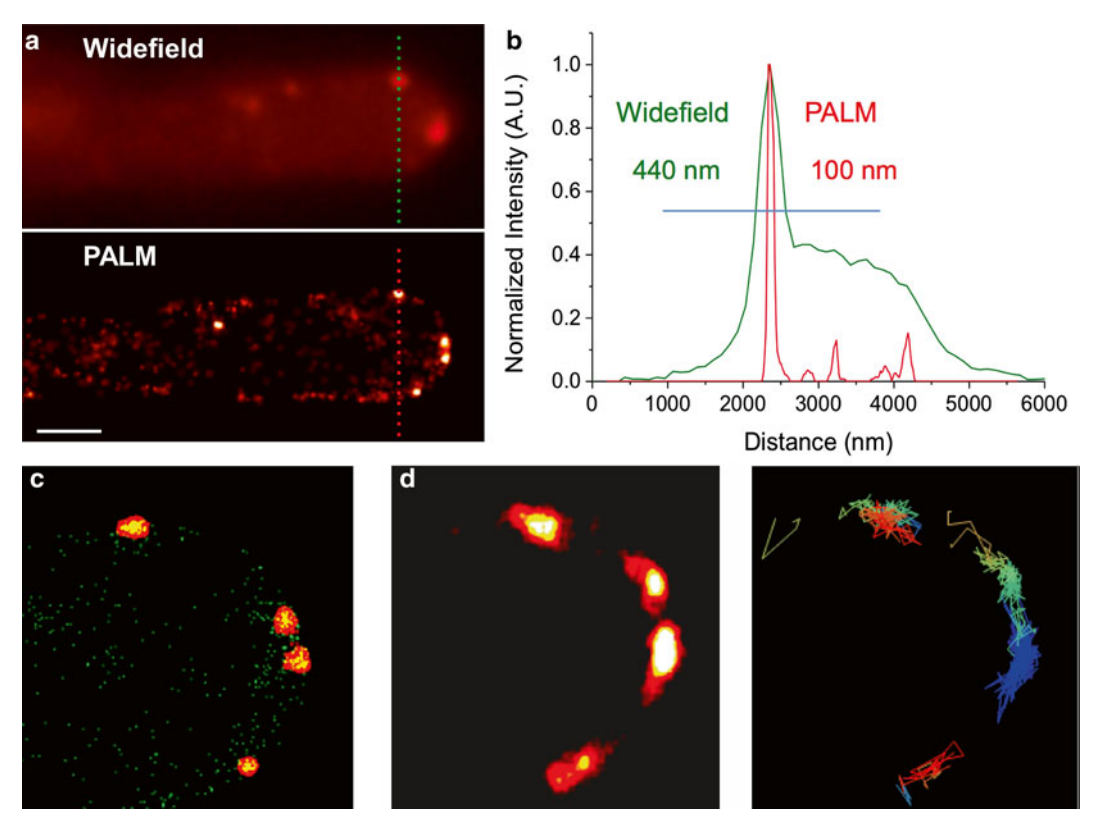


Fig. 6 PALM microscopy in *A. nidulans.* (a) Localization of mEosFP-TeaR at hyphal tip. Conventional wide-field epifluorescence microscopy (top) and PALM microscopy (bottom) are compared. The PALM micrograph is constructed by 1,000 frames with a time resolution of 50 ms ($bar = 1 \mu m$). (b) Intensity profile of a TeaR membrane domain illustrating the increased resolution achieved with PALM. Intensity was measured along the *green* and *red line* in (a). (c) Four membrane domains identified by cluster analysis (to be published elsewhere), setting the threshold on the number of neighboring molecules (ten molecules) within a certain distance r (50 nm). (d) Tracking the dynamic behavior of single molecules for a few seconds until they are photobleached. Each line indicates the movement of a single TeaR molecule. Separate *colors* indicate different molecules

Acknowledgments

We thank Dr. Stefanie Weidtkamp-Peters from the Center for Advanced Imaging (CAi) at the Heinrich-Heine University Düsseldorf for critical comments on the manuscript. Our research was in part financed by grants from the German Science Foundation through DFG/CONACYT FOR1334.

References

- 1. Harris SD (2006) Cell polarity in filamentous fungi: shaping the mold. Int Rev Cytol 251:41–77
- Riquelme M (2013) Tip growth in filamentous fungi: a road trip to the apex. Annu Rev Microbiol 67:587–609
- Read ND, Kalkman ER (2003) Does endocytosis occur in fungal hyphae? Fungal Genet Biol 39:199–203
- Penalva MA (2010) Endocytosis in filamentous fungi: Cinderella gets her reward. Curr Opin Microbiol 13:684–692
- Hervas-Aguilar A, Penalva MA (2010) Endocytic machinery protein SlaB is dispensable for polarity establishment but necessary for polarity maintenance in hyphal tip cells of *Aspergillus nidulans*. Eukaryot Cell 9:1504–1518
- Takeshita N, Mania D, Herrero S, Ishitsuka Y, Nienhaus GU, Podolski M, Howard J, Fischer R (2013) The cell-end marker TeaA and the microtubule polymerase AlpA contribute to microtubule guidance at the hyphal tip cortex of Aspergillus nidulans to provide polarity maintenance. J Cell Sci 126:5400–5411
- 7. Göhre V, Vollmeister E, Bölker M, Feldbrügge M (2012) Microtubule-dependent membrane dynamics of *Ustilago maydis*: trafficking and function of Rab5a-positive endosomes. Commun Integr Biol 5:482–487
- 8. Steinberg G (2012) The transport machinery for motility of fungal endosomes. Fungal Genet Biol 49:675–676
- Fischer R, Zekert N, Takeshita N (2008) Polarized growth in fungi – interplay between the cytoskeleton, positional markers and membrane domains. Mol Microbiol 68:813–826
- Zekert N, Fischer R (2009) The Aspergillus nidulans kinesin-3 UncA motor moves vesicles along a subpopulation of microtubules. Mol Biol Cell 20:673–684
- Penalva MA, Galindo A, Abenza JF, Pinar M, Calcagno-Pizarelli AM, Arst HN, Pantazopoulou A (2012) Searching for gold beyond mitosis: mining intracellular membrane traffic in Aspergillus nidulans. Cell Logist 2:2–14
- Vollmeister E, Schipper K, Baumann S, Haag C, Pohlmann T, Stock J, Feldbrügge M (2012) Fungal development of the plant pathogen *Ustilago maydis*. FEMS Microbiol Rev 36:59–77
- König J, Baumann S, Koepke J, Pohlmann T, Zarnack K, Feldbrügge M (2009) The fungal RNA-binding protein Rrm4 mediates long-

- distance transport of *ubi1* and *rho3* mRNAs. EMBO J 28:1855–1866
- 14. Baumann S, König J, Koepke J, Feldbrügge M (2014) Endosomal transport of septin mRNA and protein indicates local translation on endosomes and is required for correct septin filamentation. EMBO Rep 15:94–102
- Higuchi Y, Ashwin P, Roger Y, Steinberg G (2014) Early endosome motility spatially organizes polysome distribution. J Cell Biol 204: 343–357
- Todd RB, Davis MA, Hynes MJ (2007) Genetic manipulation of *Aspergillus nidulans*: heterokaryons and diploids for dominance, complementation and haploidization analyses. Nat Protoc 2:822–830
- 17. Oakley CE, Oakley BR (1989) Identification of gamma-tubulin, a new member of the tubulin superfamily encoded by mipA gene of *Aspergillus nidulans*. Nature 338:662–664
- 18. Oakley BR (2004) Tubulins in *Aspergillus nidulans*. Fungal Genet Biol 41:420–427
- 19. Morris SM, Albrecht U, Reiner O, Eichele G, Yu-Lee LY (1998) The lissencephaly gene product Lis1, a protein involved in neuronal migration, interacts with a nuclear movement protein, NudC. Curr Biol 8:603–606
- Xiang X (2003) LIS1 at the microtubule plus end and its role in dynein-mediated nuclear migration. J Cell Biol 160:289–290
- 21. Horio T, Oakley BR (2005) The role of microtubules in rapid hyphal tip growth of *Aspergillus nidulans*. Mol Biol Cell 16:918–926
- 22. Upadhyay S, Shaw BD (2008) The role of actin, fimbrin and endocytosis in growth of hyphae in *Aspergillus nidulans*. Mol Microbiol 68:690–705
- 23. Lee SC, Schmidtke SN, Dangott LJ, Shaw BD (2008) *Aspergillus nidulans* ArfB plays a role in endocytosis and polarized growth. Eukaryot Cell 7:1278–1288
- 24. Abenza JF, Galindo A, Pinar M, Pantazopoulou A, de los Rios V, Penalva MA (2012) Endosomal maturation by Rab conversion in *Aspergillus nidulans* is coupled to dynein-mediated basipetal movement. Mol Biol Cell 23:1889–1901
- Egan MJ, McClintock MA, Reck-Peterson SL (2012) Microtubule-based transport in filamentous fungi. Curr Opin Microbiol 15:637–645
- 26. Baumann S, Pohlmann T, Jungbluth M, Brachmann A, Feldbrügge M (2012) Kinesin-3 and dynein mediate microtubule-dependent

- co-transport of mRNPs and endosomes. J Cell Sci 125:2740–2752
- Betzig E, Patterson GH, Sougrat R, Lindwasser OW, Olenych S, Bonifacino JS, Davidson MW, Lippincott-Schwartz J, Hess HF (2006) Imaging intracellular fluorescent proteins at nanometer resolution. Science 313:1642–1645
- Wiedenmann J, Gayda S, Adam V, Oswald F, Nienhaus K, Bourgeois D, Nienhaus GU (2011) From EosFP to mIrisFP: structurebased development of advanced photoactivatable marker proteins of the GFP-family. J Biophotonics 4:377–390
- Takeshita N, Higashitsuji Y, Konzack S, Fischer R (2008) Apical sterol-rich membranes are essential for localizing cell end markers that determine growth directionality in the filamentous fungus Aspergillus nidulans. Mol Biol Cell 19:339–351
- 30. Li Y, Ishitsuka Y, Hedde PN, Nienhaus GU (2013) Fast and efficient molecule detection in localization-based super-resolution microscopy by parallel adaptive histogram equalization. ACS Nano 7:5207–5214

- 31. Brachmann A, König J, Julius C, Feldbrügge M (2004) A reverse genetic approach for generating gene replacement mutants in *Ustilago maydis*. Mol Genet Genomics 272:216–226
- 32. Terfrüchte M, Jöhnk B, Fajardo-Somera R, Braus G, Riquelme M, Schipper K, Feldbrügge M (2014) Establishing a versatile Golden Gate cloning system for genetic engineering in fungi. Fungal Genet Biol 62:1–10
- 33. Loubradou G, Brachmann A, Feldbrügge M, Kahmann R (2001) A homologue of the transcriptional repressor Ssn6p antagonizes cAMP signalling in *Ustilago maydis*. Mol Microbiol 40:719–730
- 34. Schneider CA, Rasband WS, Eliceiri KW (2012) NIH Image to ImageJ: 25 years of image analysis. Nat Methods 9:671–675
- 35. Kämper J, Kahmann R, Bölker M, Ma LJ, Brefort T, Saville BJ, Banuett F, Kronstad JW, Gold SE, Müller O et al (2006) Insights from the genome of the biotrophic fungal plant pathogen *Ustilago maydis*. Nature 444: 97–101